

Ligand Effects on the Structure and Magnetic Properties of Alternating Copper(II) Chains with 2,2'-Bipyrimidine- and Polymethyl-Substituted Pyrazolates as Bridging Ligands

Isabel Castro,^{*,†} M. Luisa Calatayud,[†] Wdeson P. Barros,^{†,‡} José Carranza,[§] Miguel Julve,[†] Francesc Lloret,[†] Nadia Marino,^{*,||,⊥} and Giovanni De Munno^{||}

[†]Instituto de Ciencia Molecular (ICMol)/Departament de Química Inorgànica, Universitat de València, c/José Beltrán 2, E-46980 Paterna (València), Spain

[‡]CAPES Foundation, Ministry of Education of Brazil, CEP 70040-020, Brasília, DF, Brazil

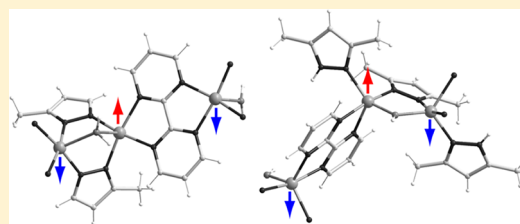
[§]Facultad de Ciencias Químicas, Universidad Autónoma de Zacatecas, Jardín Juárez s/n, 98000 Zacatecas, Mexico

^{||}Centro di Eccellenza CEMIF.CAL, Dipartimento di Chimica, Università della Calabria, via P. Bucci 14/c, 87030, Arcavacata di Rende (CS), Italy

[⊥]Department of Chemistry, Syracuse University, Syracuse, New York 13244-4100, United States

Supporting Information

ABSTRACT: A novel series of heteroleptic copper(II) compounds of formulas $\{[\text{Cu}_2(\mu\text{-H}_2\text{O})(\mu\text{-pz})_2(\mu\text{-bpm})(\text{ClO}_4)(\text{H}_2\text{O})]\text{ClO}_4 \cdot 2\text{H}_2\text{O}\}_n$ (**1**), $\{[\text{Cu}_2(\mu\text{-H}_2\text{O})(\mu\text{-3-Me}_2\text{pz})_2(\mu\text{-bpm})(\text{ClO}_4)_2 \cdot 2\text{H}_2\text{O}\}_n$ (**2**), and $\{[\text{Cu}_2(\mu\text{-OH})(\mu\text{-3,5-Me}_2\text{pz})(\mu\text{-bpm})(\text{H-3,5-Me}_2\text{pz})_2](\text{ClO}_4)_2\}_n$ (**3**) [bpm = 2,2'-bipyrimidine, Hpz = pyrazole, H-3-Me₂pz = 3-methylpyrazole, and H-3,5-Me₂pz = 3,5-dimethylpyrazole] have been synthesized and structurally characterized by X-ray diffraction methods. The crystal structures of **1** and **2** consist of copper(II) chains with regular alternating bpm and bis(pyrazolate)(aqua) bridges, whereas that of **3** is made up of copper(II) chains with regular alternating bpm and (pyrazolate)(hydroxo) bridges. The copper centers are six- (**1**) or five-coordinate (**2**) in axially elongated, octahedral (**1**) or square-pyramidal (**2**) environments in **1** and **2**, whereas they are five-coordinate in distorted trigonal-bipyramidal surroundings in **3**. The values of the copper–copper separations across the bpm/pyrazolate bridges are 5.5442(7)/3.3131(6) (**1**), 5.538(1)/3.235(1) (**2**), and 5.7673(7)/3.3220(6) Å (**3**). The magnetic properties of **1–3** have been investigated in the temperature range of 25–300 K. The analysis of their magnetic susceptibility data through the isotropic Hamiltonian for an alternating antiferromagnetic copper(II) chain model [$\mathbf{H} = -J \sum_{i=1-n/2} (\mathbf{S}_{2i} \cdot \mathbf{S}_{2i-1} + \alpha \mathbf{S}_{2i} \cdot \mathbf{S}_{2i+1})$, with $\alpha = J'/J$ and $S_i = S_{\text{Cu}} = 1/2$] reveals the presence of a strong to moderate antiferromagnetic coupling through the bis(pyrazolate)(aqua) [$-J = 217$ (**1**) and 215 cm^{-1} (**2**)] and (pyrazolate)(hydroxo) bridges [$-J = 153 \text{ cm}^{-1}$ (**3**)], respectively, whereas a strong to weak antiferromagnetic coupling occurs through the bis-bidentate bpm [$-J' = 211$ (**1**), 213 (**2**), and 44 cm^{-1} (**3**)]. A simple orbital analysis of the magnetic exchange interaction within the bpm- and pyrazolate-bridged dicopper(II) fragments of **1–3** visualizes the σ -type pathways involving the (dx^2-y^2) (**1** and **2**) or $d(z^2)$ (**3**) magnetic orbitals on each metal ion, which account for the variation of the magnetic properties in these three novel examples of one-dimensional copper(II) compounds with regular alternating intrachain antiferromagnetic interactions.



INTRODUCTION

Magnetic chain compounds were actively investigated in the field of molecular magnetism as models for one-dimensional spin arrays, from both experimental and theoretical points of views.¹ A simple reason for this interest is that they offer the possibility to solve exactly some relevant physical problems in one dimension (1D) that are too complex to be solved in three dimensions (3D), opening thus a new chapter of low-dimensional magnetism in the wide discipline of low-dimensional physics.² Because of the possibility to achieve a long-range magnetic ordering through interchain interactions, they were also studied having in mind the design and synthesis of molecular-based magnets.³ The recent finding of magnetic

hysteresis effects in 1D compounds, which are not associated with a 3D magnetic order but to a slow magnetic relaxation, has provided an experimental confirmation of Glauber's prediction and opened exciting new perspectives of storing information in low-dimensional magnetic materials.⁴

In the zoo of magnetic chain compounds, homometallic (either uniform or alternating) antiferromagnetic chains are relatively common systems with current interest in spin dynamics and quantum critical phenomena.^{2e} In that respect, an important difference in the quantum description of

Received: March 13, 2014

Published: May 14, 2014

homometallic uniform antiferromagnetic chains resides on the value of the spin, half-integer (fermions) or integer (bosons). Therefore, there exists an energy gap between the ground singlet spin state and the first excited (triplet) spin state in integer spin 1D systems.^{1a} This quantum effect known as Haldane's conjecture was experimentally observed in uniform $S = 1$ Ni^{II} antiferromagnetic chains.⁵ On the contrary, half-integer spin 1D systems, such as uniform $S = 1/2$ Cu^{II} antiferromagnetic chains, possess a gapless excitation spectrum with a ground singlet spin state infinitely close to the first excited states.^{1a} An important magnetic quantum phenomenon related to this point is the spin-Peierls transition that occurs when a uniform antiferromagnetic chain becomes an alternating one because of the coupling between the vibrations (phonons) of the lattice and the exchange energy.^{1a} Dimerization of spins leads to a modification of the excitation spectrum in the resulting alternating $S = 1/2$ Cu^{II} antiferromagnetic chains,⁶ which have recently emerged as models for the study of the quantum entanglement phenomenon.⁷

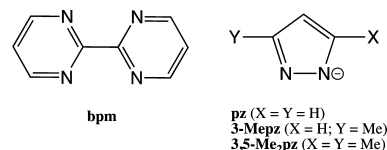
In this context, homometallic 1D systems containing different bridging moieties deserve particular attention because alternating magnetic couplings differing in sign and/or magnitude can occur, depending on the nature of the bridging ligands.⁸ In that respect, copper(II) chains with two alternating intrachain antiferromagnetic interactions (J and $J' < 0$) are well-known, whereas those with alternating antiferro- and ferromagnetic interactions of different sign ($J < 0$ and $J' > 0$) are still fairly uncommon.⁹ During the last two decades, our research group has been particularly interested in the magnetochemistry of copper(II) chain compounds, both uniform and alternating ones, with a variety of bridging ligands.^{10–23} For instance, we reported the first examples of regular alternating antiferro/ferromagnetic interactions in copper(II) chains across 2,2'-bipyrimidine (bpm) and hydroxo bridges.^{10a,d} This pioneering work has been recently extended to analogous alternating antiferromagnetic copper(II) chains with bpm and fluoride bridges.^{10f} In both cases, the bpm molecule adopts a bis-bidentate coordination mode, and it mediates antiferromagnetic exchange interactions between the unpaired electrons of the Cu^{II} ions, while either ferro- or antiferromagnetic exchange couplings occur across the double hydroxo and fluoride bridges, respectively.^{10a,d,f}

Inspired by these results, we have turned our attention to pyrazolate (pz) as an additional bridging ligand in order to explore the possibility to get antiferromagnetic copper(II) chains with regular alternating bpm and pz bridges. In fact, earlier studies on homoleptic pyrazolate coordination polymers with first row transition-metal ions demonstrated that the anion of pyrazole often adopts the N,N' -bridging coordination to metal ions, this pathway having a remarkable ability to mediate strong antiferromagnetic exchange interactions between paramagnetic centers.^{24,25} The interest in these low-dimensional magnetic materials stems from the expectation that they provide unique examples of uniform copper(II) chains with strong antiferromagnetic interactions across the pyrazolate bridges.^{24a} By varying the substituents on the pyrazolate ring, it has been possible to examine systematically how the structures and magnetic properties of the isolated compounds are influenced by the steric and electronic factors.^{24b,c}

The present work concerns the syntheses and general physical characterization, X-ray structures, and magnetic studies of a novel series of heteroleptic copper(II) compounds with bpm and the pz anion or its 3-methyl-(3-Mepz) and 3,5-

dimethyl-substituted (3,5-Me₂pz) derivatives as bridging ligands (Chart 1). Our goal is to investigate the influence of

Chart 1. Chemical Structures of Bipyrimidine- and Polymethyl-Substituted Pyrazolates Used as Bridging Ligands



the steric and/or electronic effects of the ligand on the structural and magnetic properties of this unique family of mixed bpm and polymethyl-substituted pyrazolate copper(II) compounds, namely, $\{[\text{Cu}_2(\mu\text{-H}_2\text{O})(\mu\text{-pz})_2(\mu\text{-bpm})(\text{ClO}_4)(\text{H}_2\text{O})](\text{ClO}_4)_2 \cdot 2\text{H}_2\text{O}\}_n$ (**1**), $\{[\text{Cu}_2(\mu\text{-H}_2\text{O})(\mu\text{-3-Mepz})_2(\mu\text{-bpm})](\text{ClO}_4)_2 \cdot 2\text{H}_2\text{O}\}_n$ (**2**), and $\{[\text{Cu}_2(\mu\text{-OH})(\mu\text{-3,5-Me}_2\text{pz})(\mu\text{-bpm})(\text{H-3,5-Me}_2\text{pz})_2](\text{ClO}_4)_2\}_n$ (**3**). Compounds **1–3** are three novel examples of alternating bpm- and pz-, 3-Mepz-, or 3,5-Me₂pz-bridged copper(II) chains with exogenous water or hydroxide as additional bridges. Although a large number of bipyrimidine- and pyrazolate-bridged dinuclear copper(II) complexes have been reported in the literature and magnetostructural correlations for them are well-established,^{26–28} no examples of alternating copper(II) chains bearing both types of bridges have been reported so far. Therefore, the nature and magnitude of the distinct intrachain magnetic couplings for **1–3** are discussed in the light of their different exchange pathways and compared with those reported for the related bpm-²⁶ and mono-²⁷ or bis(pyrazolate)-bridged^{27t,u,28} dicopper(II) complexes.

EXPERIMENTAL SECTION

Materials and Methods. 2,2'-Bipyrimidine, pyrazole, 3-methylpyrazole, 3,5-dimethylpyrazole, copper(II) perchlorate hexahydrate, and the organic base triethylamine were purchased from commercial sources and used as received. The elemental (C, H, N) and electron microscopy (Cu, Cl) analyses were performed by the Servicio Interdepartamental de la Universidad de Valencia. Infrared spectra were recorded on a Bruker IF555 spectrometer as KBr pellets.

Caution! Perchlorate salts of metal complexes with organic ligands are potentially explosive. We worked at the mmol scale, and the starting perchlorate salt was an aquo complex. The diluted solutions were handled with care and evaporated slowly at room temperature in an open hood.

Preparation of the Compounds. $\{[\text{Cu}_2(\mu\text{-H}_2\text{O})(\mu\text{-pz})_2(\mu\text{-bpm})(\text{ClO}_4)(\text{H}_2\text{O})](\text{ClO}_4)_2 \cdot 2\text{H}_2\text{O}\}_n$ (**1**), $\{[\text{Cu}_2(\mu\text{-H}_2\text{O})(\mu\text{-3-Mepz})_2(\mu\text{-bpm})](\text{ClO}_4)_2 \cdot 2\text{H}_2\text{O}\}_n$ (**2**), and $\{[\text{Cu}_2(\mu\text{-OH})(\mu\text{-3,5-Me}_2\text{pz})(\mu\text{-bpm})(\text{H-3,5-Me}_2\text{pz})_2](\text{ClO}_4)_2\}_n$ (**3**). A similar synthetic procedure was used for the preparation of all three complexes. Bpm (0.074 g, 1/2 mmol) dissolved in a minimum amount of water (10 mL) was slowly added to an aqueous solution (15 mL) of copper(II) perchlorate hexahydrate (0.370 g, 1 mmol). The addition of Hpz (**1**) (0.068 g, 1 mmol), H-3-Mepz (**2**) (0.082 g, 1 mmol), or H-3,5-Me₂pz (**3**) (0.096 g, 1 mmol) caused a color change from green to blue. The blue color of each solution was enhanced when an aqueous solution (20 mL) of triethylamine (0.101 g, 1 mmol) was poured into the solution under continuous stirring. The resulting solutions were filtered off to remove any small solid particle and allowed to evaporate at room temperature in a hood. X-ray quality dark green polyhedral crystals of **1** and **2** were grown from their corresponding solutions after a few days, which were collected by filtration, washed with a small amount of cold water, and dried on filter paper. Suitable X-ray crystals of **3** as green parallelepipeds were grown from its solution after several days, together with a minor amount of blue crystals of a monomeric

Table 1. Summary of Crystal Data for 1–3

	1	2	3
formula	C ₁₄ H ₂₀ Cl ₂ Cu ₂ N ₈ O ₁₂	C ₁₆ H ₂₂ Cl ₂ Cu ₂ N ₈ O ₁₁	C ₂₃ H ₃₀ Cl ₂ Cu ₂ N ₁₀ O ₉
M _r	690.36	700.40	788.55
crystal system	orthorhombic	orthorhombic	orthorhombic
space group	P2 ₁ 2 ₁ 2 ₁	Fdd2	Pbca
a/Å	12.5983(9)	26.3979(18)	18.4099(17)
b/Å	13.4940(13)	27.717(3)	15.6527(14)
c/Å	15.2415(14)	15.3681(18)	22.408(2)
β/deg	90	90	90
V/Å ³	2591.1(4)	11244(2)	6457.1(10)
Z	4	16	8
D _c /g cm ⁻³	1.770	1.655	1.547
T/K	296(2)	296(2)	296(2)
F(000)	1392	5664	3216
μ(Mo–Kα)/mm ⁻¹	1.770	1.768	1.547
reflns. collected	34 666	44 191	134 748
reflns. indep. (R _{int})	5290 (0.0306)	5019 (0.0740)	5910 (0.0426)
reflns. obs. [I > 2σ(I)]	5013	4284	4581
R ₁ ^a [I > 2σ(I)] (all)	0.0388 (0.0423)	0.0595 (0.0700)	0.0436 (0.0603)
wR ₂ ^b [I > 2σ(I)] (all)	0.1166 (0.1192)	0.1715 (0.1819)	0.1124 (0.1233)
goodness-of-fit on F ²	1.052	1.121	1.046
abs. struct. param.	0.23(2)	0.40(3)	
Δρ _{max,min} /e·Å ⁻³	0.762 and -0.597	1.103 and -0.464	0.689 and -0.530

^aR₁ = Σ(|F_o| - |F_c|) / Σ|F_o|. ^bwR₂ = {Σ[w(F_o² - F_c²)²] / Σ[w(F_o²)²]}^{1/2} and w = 1/[σ²(F_o²) + (mP)² + nP] with P = (F_o² + 2F_c²)/3, m = 0.0955 (1), 0.1314 (2), and 0.0557 (3), and n = 0.4008 (1), 2.6843 (2), and 11.0309 (3).

Table 2. Selected Interatomic Bond Lengths (Å) and Angles (deg) for 1^a

Cu(1)–N(1)	2.068(3)	Cu(2)–N(6)	1.963(3)
Cu(1)–N(3)	2.077(3)	Cu(2)–N(8)	1.967(3)
Cu(1)–N(5)	1.956(3)	Cu(2)–N(2a)	2.089(3)
Cu(1)–N(7)	1.956(3)	Cu(2)–N(4a)	2.058(3)
Cu(1)–O(1w)	2.445(3)	Cu(2)–O(1w)	2.299(3)
Cu(1)–O(2w)	2.476(5)	Cu(2)–O(1)	2.65(1)
N(1)–Cu(1)–N(3)	80.00(12)	N(6)–Cu(2)–N(8)	91.69(13)
N(1)–Cu(1)–N(5)	93.38(13)	N(6)–Cu(2)–N(2a)	170.27(12)
N(1)–Cu(1)–N(7)	173.97(14)	N(6)–Cu(2)–N(4a)	93.41(13)
N(1)–Cu(1)–O(1w)	89.86(12)	N(6)–Cu(2)–O(1w)	91.62(12)
N(1)–Cu(1)–O(2w)	86.84(18)	N(6)–Cu(2)–O(1)	83.2(3)
N(3)–Cu(1)–N(5)	173.29(13)	N(8)–Cu(2)–N(2a)	94.40(13)
N(3)–Cu(1)–N(7)	94.48(13)	N(8)–Cu(2)–N(4a)	173.45(12)
N(3)–Cu(1)–O(1w)	91.88(13)	N(8)–Cu(2)–O(1w)	90.88(13)
N(3)–Cu(1)–O(2w)	85.967(19)	N(8)–Cu(2)–O(1)	91.4(4)
N(5)–Cu(1)–N(7)	92.19(14)	N(2a)–Cu(2)–N(4a)	80.02(12)
N(5)–Cu(1)–O(1w)	89.19(13)	N(2a)–Cu(2)–O(1w)	95.87(12)
N(5)–Cu(1)–O(2w)	92.91(19)	N(2a)–Cu(2)–O(1)	89.1(3)
N(7)–Cu(1)–O(1w)	87.90(12)	N(4a)–Cu(2)–O(1w)	93.03(13)
N(7)–Cu(1)–O(2w)	95.20(19)	N(4a)–Cu(2)–O(1)	85.1(3)
O(1w)–Cu(1)–O(2w)	176.18(18)	O(1w)–Cu(2)–O(1)	174.3(4)
Cu(1)–O(1w)–Cu(2)	88.54(10)		

^aSymmetry operation used to generate equivalent atoms: (a) = -x + 3/2, -y + 2, z - 1/2.

impurity (data reported elsewhere), which were separated by hand and air-dried. Yield ca. 62% (1), 58% (2), and 31% (3). Anal. Calcd for Cu₂C₁₄H₂₀N₈O₁₂Cl₂ (1): C, 24.36; H, 2.92; N, 16.23. Found: C, 24.26; H, 3.01; N, 16.11%. Anal. Calcd for Cu₂C₁₆H₂₂N₈O₁₁Cl₂ (2): C, 27.44; H, 3.17; N, 16.00. Found: C, 26.88; H, 3.36; N, 15.62%. Anal. Calcd for Cu₂C₂₃H₃₀N₁₀O₉Cl₂ (3): C, 34.90; H, 3.83; N, 17.79. Found: C, 35.02; H, 3.84; N, 17.77%. Electron microscopy analyses: 1:1 Cu:Cl molar ratio for 1–3. IR (cm⁻¹): 3447s (O–H from water), 1593s (C=N from bis-bidentate bpm),^{10b} 1500m (C=N from bis-monodentate pyrazolate),^{27t} and 1084vs (Cl–O from perchlorate) for 1; 3396s (O–H from water), 1593s (C=N from bis-bidentate

bpm),^{10b} 1505m (C=N from bis-monodentate pyrazolate),^{27t} and 1098vs (Cl–O from perchlorate) for 2; 3600m (O–H from hydroxide),²⁹ 3236m (N–H from monodentate pyrazole),^{27t} 1593s (C=N from bis-bidentate bpm),^{10b} 1534m (C=N from monodentate pyrazole),^{27t} 1500m (C=N from bis-monodentate pyrazolate),^{27t} and 1120vs (Cl–O from perchlorate) for 3.

Magnetic Measurements. Variable-temperature magnetic susceptibility measurements under applied dc fields of 1 T (100 ≤ T ≤ 300 K) and 1000 G (25 ≤ T < 100 K) were carried out on powdered samples of 1–3 with a SQUID magnetometer. Diamagnetic corrections for the constituent atoms were made by using the Pascal's

Table 3. Selected Interatomic Bond Lengths (Å) and Angles (deg) for 2^a

Cu(1)–N(1)	2.113(6)	Cu(2)–N(8)	1.938(6)
Cu(1)–N(3)	2.034(7)	Cu(2)–N(6)	1.995(6)
Cu(1)–N(5)	1.951(6)	Cu(2)–N(2a)	2.111(6)
Cu(1)–N(7)	1.987(6)	Cu(2)–N(4a)	2.044(6)
Cu(1)–O(1w)	2.293(5)	Cu(2)–O(1w)	2.303(6)
N(1)–Cu(1)–N(3)	80.0(2)	N(8)–Cu(2)–N(6)	91.6(3)
N(1)–Cu(1)–N(5)	93.9(3)	N(6)–Cu(2)–N(2a)	171.3(2)
N(1)–Cu(1)–N(7)	170.9(2)	N(6)–Cu(2)–N(4a)	94.2(3)
N(1)–Cu(1)–O(1w)	95.3(2)	N(6)–Cu(2)–O(1w)	92.0(2)
N(3)–Cu(1)–N(5)	172.5(3)	N(8)–Cu(2)–N(2a)	94.2(2)
N(3)–Cu(1)–N(7)	94.5(2)	N(8)–Cu(2)–N(4a)	172.0(2)
N(3)–Cu(1)–O(1w)	93.4(2)	N(8)–Cu(2)–O(1w)	90.9(2)
N(5)–Cu(1)–N(7)	91.0(3)	N(2a)–Cu(2)–O(1w)	94.4(2)
N(5)–Cu(1)–O(1w)	91.5(2)	N(4a)–Cu(2)–N(2a)	79.5(2)
N(7)–Cu(1)–O(1w)	92.2(2)	N(4a)–Cu(2)–O(1w)	94.5(2)
Cu(1)–O(1w)–Cu(2)	89.5(2)		

^aSymmetry operation used to generate equivalent atoms: (a) = $-x, -y - 3/2, z + 1/2$.

Table 4. Selected Interatomic Bond Lengths (Å) and Angles (deg) for 3^a

Cu(1)–N(1)	2.056(3)	Cu(2)–N(2a)	2.227(3)
Cu(1)–N(3)	2.309(3)	Cu(2)–N(4a)	2.063(3)
Cu(1)–N(5)	1.957(3)	Cu(2)–N(6)	1.958(3)
Cu(1)–N(7)	2.031(3)	Cu(2)–N(9)	2.077(3)
Cu(1)–O(9)	1.904(3)	Cu(2)–O(9)	1.914(3)
N(1)–Cu(1)–N(3)	75.7(1)	N(2a)–Cu(2)–N(4a)	76.8(1)
N(1)–Cu(1)–N(5)	166.5(1)	N(2a)–Cu(2)–N(6)	91.0(1)
N(1)–Cu(1)–N(7)	89.7(1)	N(2a)–Cu(2)–N(9)	112.7(1)
N(1)–Cu(1)–O(9)	93.5(1)	N(2a)–Cu(2)–O(9)	124.0(1)
N(3)–Cu(1)–N(5)	90.9(1)	N(4a)–Cu(2)–N(6)	166.0(1)
N(3)–Cu(1)–N(7)	114.3(1)	N(4a)–Cu(2)–N(9)	93.5(1)
N(3)–Cu(1)–O(9)	109.6(1)	N(4a)–Cu(2)–O(9)	93.0(1)
N(5)–Cu(1)–N(7)	97.5(1)	N(6)–Cu(2)–N(9)	97.6(1)
N(5)–Cu(1)–O(9)	89.3(1)	N(6)–Cu(2)–O(9)	88.2(1)
N(7)–Cu(1)–O(9)	135.4(1)	N(9)–Cu(2)–O(9)	122.9(1)
Cu(1)–O(9)–Cu(2)	120.9(1)		

^aSymmetry operation used to generate equivalent atoms: (a) = $-x + 3/2, y + 1/2, z$.

constants. The experimental data were also corrected for the temperature-independent paramagnetism of the metal center [$120 \times 10^{-6} \text{ cm}^3 \text{ mol}^{-1}$ per two copper(II) ions] and the sample holder (a plastic bag).

X-ray Crystallographic Analysis. X-ray diffraction data for 1–3 were collected with a Bruker-Nonius X8APEXII CCD area detector diffractometer using graphite-monochromated Mo- $K\alpha$ radiation ($\lambda = 0.71073 \text{ \AA}$). The data were processed through the SAINT³⁰ reduction and SADABS³¹ absorption software. A summary of the crystallographic data and structure refinement for 1–3 is given in Table 1. The structures of 1–3 were solved by direct methods using SHELXS, and they were refined against F^2 on all data by full-matrix least-squares with SHELXL-97³² through established methods.³³ All non-hydrogen atoms except the oxygen atoms of the water molecules of crystallization in 1 [O(3w) and O(4w)] and 2 [O(2w) and O(3w)] were refined anisotropically. The hydrogen atoms of the bridging water molecule in 1 and 2 [O(1w)], as well as that of the bridging hydroxo group in 3 [O(9)], were located on a ΔF map and refined with restraints. The hydrogen atoms on the terminal water molecule in 1 [O(2w)] and those belonging to the water molecules of crystallization in 1 and 2 were not defined. The hydrogen atoms of the pyrazolate and bpm molecules were set in calculated positions and refined by using a riding model. All the perchlorate anions in 1–3 were found disordered, and they were modeled over two sites. The relative occupancies of the two atomic sets were refined freely within SHELXL, while constraining the sum of the occupancies to unity.³³ All

disorders were refined using similarity restraints on 1,2- and 1,3-distances and rigid-bond restraints.³³ Similar anisotropic displacement parameters (ADP)³³ were also applied in some cases. The final full-matrix least-squares refinements on F^2 , minimizing the function $\sum w(|F_o| - |F_c|)^2$, reached convergence with the values of the discrepancy indices given in Table 1. Selected bond distances and interbond angles for 1–3 are listed in Tables 2–4. Graphical manipulations were performed with either the XP utility of the SHELXTL system or the Diamond program.³⁴ CCDC reference numbers 987579–987581 (1–3). See the Supporting Information for crystallographic data in CIF format.

RESULTS AND DISCUSSION

Synthesis. The cationic copper(II) chains of general formulas $\{[\text{Cu}_2(\mu\text{-H}_2\text{O})(\mu\text{-L})_2(\mu\text{-bpm})(\text{ClO}_4)_m(\text{H}_2\text{O})_m]^{(2-m)+}\}_n$ [L = pz (1) and 3-Mepz (2) with $m = 1$ (1) and 0 (2)] and $\{[\text{Cu}_2(\mu\text{-OH})(\mu\text{-L})(\mu\text{-bpm})(\text{HL})_2]^{2+}\}_n$ [L = 3,5-Me₂pz (3)] were synthesized by the reaction of copper(II) perchlorate/HL/bpm (2:2:1 molar ratio) in water using the stoichiometric amount of triethylamine that is needed to deprotonate the pyrazole ligands. However, the pyrazole moieties in 3 are present as both bridging pyrazolate and terminal pyrazole ligands, while a counterbalancing hydroxide anion is present as an additional exogenous bridging ligand.

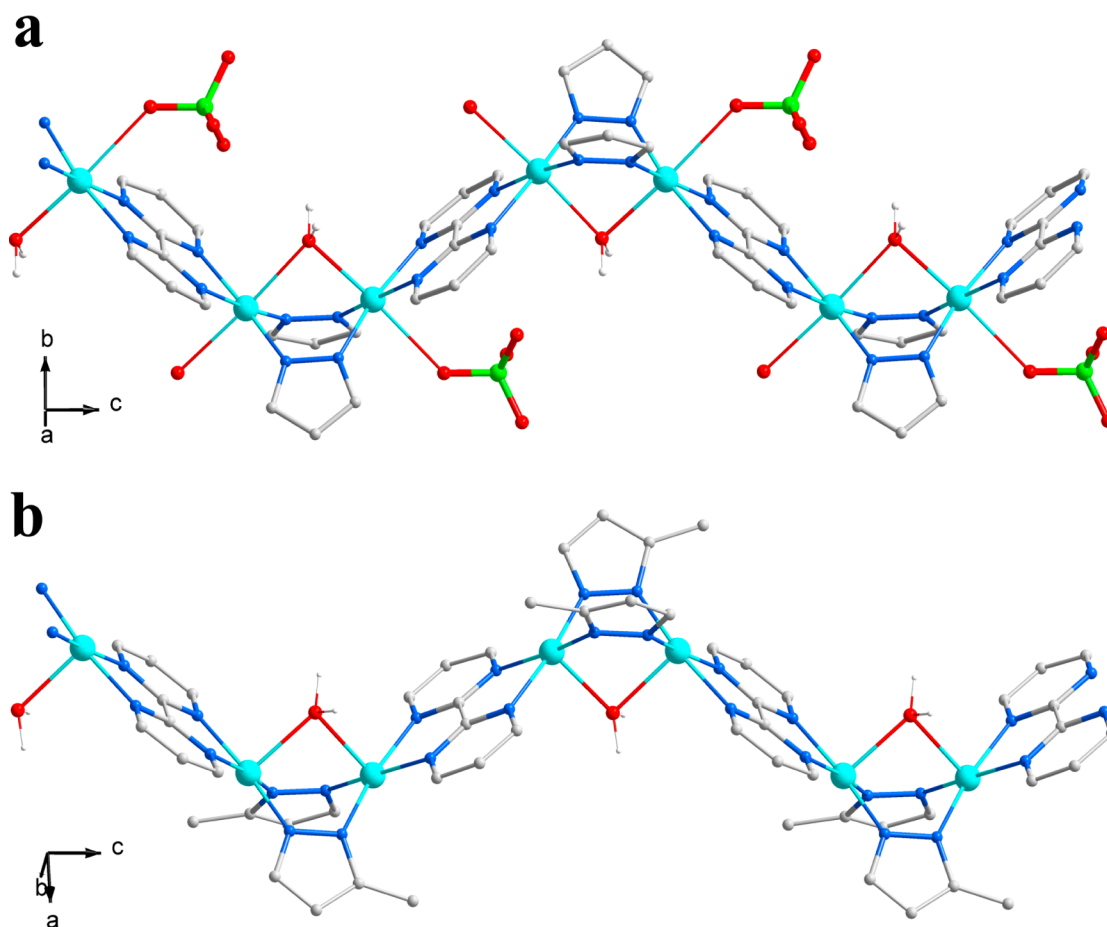


Figure 1. Perspective views of a fragment of the wavelike cationic $\{[\text{Cu}_2(\mu\text{-H}_2\text{O})(\mu\text{-pz})_2(\mu\text{-bpm})(\text{ClO}_4)(\text{H}_2\text{O})]^+\}_n$ and $\{[\text{Cu}_2(\mu\text{-H}_2\text{O})(\mu\text{-3-Mepz})_2(\mu\text{-bpm})]^{2+}\}_n$ chain motifs in **1** (a) and **2** (b), respectively.

Compounds **1–3** were isolated as their perchlorate salts in the form of green crystals with good to moderate yields [62% (**1**), 58% (**2**), and 31% (**3**)] after a few days under slow evaporation at room temperature.

The formation of **1** and **2** upon changing pz by 3-Mepz indicates that the steric constraints of the methyl group are small, if not negligible. Conversely, the occurrence of different protonation degrees for the dimethyl-substituted pyrazole/pyrazolate moieties in **3**, when compared to the situation found for **1** and **2**, would be likely explained by the electron-donating character of the methyl group that enhances the basicity of the pyrazolate donor group, disfavoring thus its deprotonation. The chemical identity of **1–3** was established by elemental and electron microscopy analyses and infrared spectroscopy (see the Experimental Section), and it was further confirmed by single-crystal X-ray diffraction.

Description of the Structures. $\{[\text{Cu}_2(\mu\text{-H}_2\text{O})(\mu\text{-pz})_2(\mu\text{-bpm})(\text{ClO}_4)(\text{H}_2\text{O})]\text{ClO}_4 \cdot 2\text{H}_2\text{O}\}_n$ (**1**) and $\{[\text{Cu}_2(\mu\text{-H}_2\text{O})(\mu\text{-3-Mepz})_2(\mu\text{-bpm})](\text{ClO}_4)_2 \cdot 2\text{H}_2\text{O}\}_n$ (**2**). The crystal structures of **1** and **2** consist of wavelike cationic copper(II) chains of the general formula $\{[\text{Cu}_2(\mu\text{-H}_2\text{O})(\mu\text{-L})_2(\mu\text{-bpm})(\text{ClO}_4)_m(\text{H}_2\text{O})_m]^{(2-m)+}\}_n$ [$\text{L} = \text{pz}$ (**1**) and 3-Mepz (**2**) with $m = 1$ (**1**) and 0 (**2**)], featuring regular alternating bpm (**1** and **2**) and triple bis(pyrazolate)(aqua) or bis(3-methylpyrazolate)(aqua) (**2**) bridges, together with uncoordinated and/or weakly coordinated perchlorate anions, and crystallization water molecules. The values of the copper–copper distances across the bpm/L [$\text{L} = \text{pz}$ (**1**) and 3-Mepz (**2**)] bridges are

5.5442(7)/3.3131(6) (**1**) and 5.538(1)/3.235(1) Å (**2**). A view of a fragment of these two chains is shown in Figure 1.

The two crystallographically independent copper(II) ions in **1** [Cu(1) and Cu(2)] have an axially elongated octahedral geometry, whereas the corresponding ones in **2** can be described as square-pyramidal with values of the trigonality parameter (τ) of 0.03 at Cu(1) and 0.01 at Cu(2) [$\tau = 0$ and 1 for square-pyramidal and trigonal-bipyramidal surroundings, respectively]³⁵ (Figures 2 and 3). The equatorial/basal planes of the CuN_4O_2 (**1**) and CuN_4O (**2**) coordination environments are built up by four imine nitrogen atoms from the bis(bidentate) bpm and the two bis(monodentate) pz (**1**) and 3-Mepz (**2**) ligands. The oxygen atom of the bridging water molecule occupies one axial position of the copper(II) ions in **1** or the apical position in **2**. The coordination sphere of Cu(1) and Cu(2) in **1** is completed by either a water molecule [Cu(1)–O(2w) = 2.476(5) Å] or a weakly coordinated perchlorate oxygen atom [Cu(2)–O(1) = 2.65(1) Å]. It seems reasonable to assume that these differences in the coordination geometry of the metal atoms in **1** and **2** (i.e., six- vs five-coordination) are somehow due to the steric hindrance of the methyl substituent on the 3-Mepz ligands in **2**.

The equatorial Cu–N_{bpm} bond distances [Cu–N = 2.058(3)–2.089(3) Å (**1**) and 2.033(7)–2.114(6) Å (**2**)] are greater than the Cu–N_{pz} ones [Cu–N = 1.956(3)–1.967(3) Å (**1**) and 1.937(6)–1.996(6) Å (**2**)], both being shorter than the axial/apical Cu–O_w and/or Cu–O_{perchlorate} bond distances in **1** and **2** (see Tables 2 and 3), as expected for a Jahn–Teller

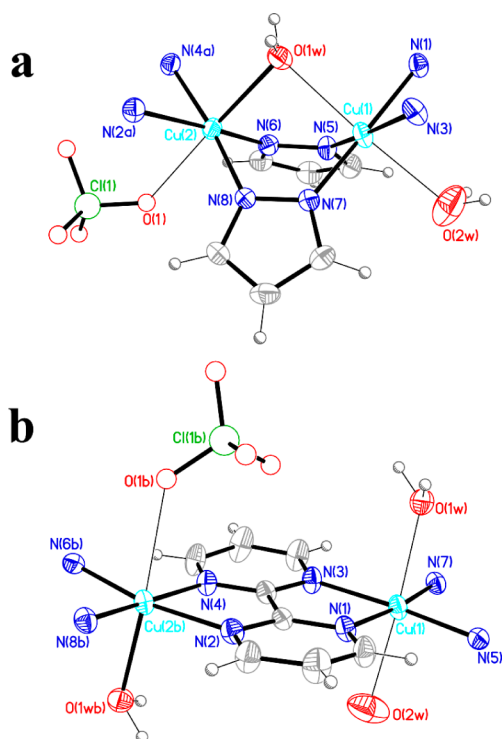


Figure 2. Comparative views of the two alternating bridging moieties in **1**, showing the atom numbering: (a) bis(μ -pyrazolate)(μ -aqua)-dicopper(II) and (b) (μ -bipyrimidine)dicopper(II) units. Only the major disorder set is represented for the weakly coordinated perchlorate group, for clarity. Thermal ellipsoids are drawn at the 30% probability level. Symmetry operations used to generate equivalent atoms: (a) = $-x + 3/2, -y + 2, z - 1/2$; (b) = $-x + 3/2, -y + 2, z + 1/2$.

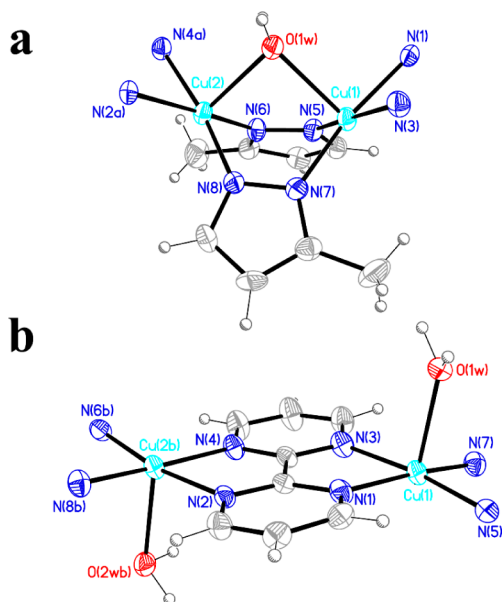


Figure 3. Comparative views of the two alternating bridging moieties in **2**, showing the atom numbering: (a) bis(μ -3-methylpyrazolate)(μ -aqua)dicopper(II) and (b) (μ -bipyrimidine)dicopper(II) units. Thermal ellipsoids are drawn at the 30% probability level. Symmetry operations used to generate equivalent atoms: (a) = $-x, -y - 3/2, z + 1/2$; (b) = $-x, -y - 3/2, z - 1/2$.

distorted octahedral or square-pyramidal d^9 Cu^{II} ion. The Cu(1) atom in **1** lays basically on the equatorial plane, whereas Cu(2) is slightly shifted toward the bridging water molecule [mean displacements (h_{M}) being $-0.012(1)$ and $0.098(2)$ Å, respectively]. Both metal atoms in **2** are slightly shifted toward the bridging water molecule by ca. $0.10(1)$ Å.

The mean planes of the pz (**1**) and 3-Mepz (**2**) ligands within the $[\text{Cu}^{\text{II}}_2(\mu\text{-H}_2\text{O})(\mu\text{-pz})_2]$ (**1**) and $[\text{Cu}^{\text{II}}_2(\mu\text{-H}_2\text{O})(\mu\text{-3-Mepz})_2]$ (**2**) fragments are neither coplanar with each other nor coplanar with the equatorial/basal planes of the copper(II) ions (Figures 2a and 3a). The values of the dihedral angle between the mean basal planes at the copper atoms and the mean planes of the pyrazolate groups (ψ) are in the ranges $53.8(2)$ – $58.7(2)^\circ$ (**1**) and $56.9(3)$ – $60.4(3)^\circ$ (**2**), whereas the values of the dihedral angle between the mean pyrazolate planes (θ) are $80.3(2)^\circ$ (**1**) and $89.5(3)^\circ$ (**2**). This situation leads to an overall bent conformation of the resulting six-membered metallacyclic core at the dicopper(II)bis-(pyrazolate)(aqua)-bridging unit in **1** and **2**, as previously found for the similar triply bis(pyrazolate)(halide)-bridged dinuclear copper(II) complexes of formulas $\text{PPh}_4[\text{Cu}_2(\mu\text{-Cl})(\mu\text{-pz})_2\{\text{H}_2\text{B}(\text{pz})_2\}_2] \cdot 0.5\text{Me}_2\text{CO}$ and $\text{AsPh}_4[\text{Cu}_2(\mu\text{-Br})(\mu\text{-pz})_2\{\text{H}_2\text{B}(\text{pz})_2\}_2] \cdot \text{Me}_2\text{CO}$ [PPh_4^+ = tetraphenylphosphonium, AsPh_4^+ = tetraphenylarsonium, and $\text{H}_2\text{B}(\text{pz})_2^-$ = dihydrobis(1-pyrazolyl)borate].^{28a} The values of the dihedral angle between the mean equatorial/basal planes at the copper(II) ions (ϕ) are $84.7(1)^\circ$ (**1**) and $85.6(2)^\circ$ (**2**). The putative role of the exogenous bridging ligand in the occurrence of this unique bent conformation of the $[\text{Cu}^{\text{II}}_2(\mu\text{-H}_2\text{O})(\mu\text{-pz})_2]$ (**1**) and $[\text{Cu}^{\text{II}}_2(\mu\text{-H}_2\text{O})(\mu\text{-3-Mepz})_2]$ (**2**) fragments is unclear, because the same conformation is also common to a related series of doubly bis(pyrazolate)-bridged dinuclear copper(II) complexes with no additional supporting bridge of general formulas $[\text{Cu}_2\text{L}_2\text{L}'_2](\text{NO}_3)_2 \cdot n\text{H}_2\text{O}$ [L = pyrazolate (pz), 4-methylpyrazolate (4-Mepz), 4-chloropyrazolate (4-Clpz), and 4-bromopyrazolate (4-Brpz); L' = 2,2'-bipyridine (bpy) and 1,10-phenanthroline (phen); $n = 0-2$].^{28b}

As far as the $[\text{Cu}^{\text{II}}_2(\mu\text{-bpm})]$ fragment in **1** and **2** is concerned, the atoms filling the equatorial/basal positions at the copper(II) ions are basically coplanar as the bpm ligand itself (Figures 2b and 3b). The values of the dihedral angle between the former and the latter planes (ψ') are in the ranges of $5.1(2)$ – $8.5(2)^\circ$ (**1**) and $9.0(3)$ – $12.3(3)^\circ$ (**2**), whereas those of the dihedral angle between the former planes across the bpm bridge (ϕ') are $3.6(2)^\circ$ (**1**) and $4.2(3)^\circ$ (**2**). This situation leads to an overall planar conformation of the (μ -bpm)-dicopper(II) entity in **1** and **2**.

Neighboring chains in the crystal lattice of **1** and **2** define intersected supramolecular layers orthogonal to the crystallographic ab plane by means of an intricate network of hydrogen bonds involving the coordinated and uncoordinated water molecules [$\text{O}_{\text{w}}-\text{H}\cdots\text{O}_{\text{w}}$ distances of ca. $2.7(1)$ – $2.8(1)$ Å; see Tables S1 and S2, Supporting Information], as well as the perchlorate counteranions (Figure S1, Supporting Information). Although the general structural scaffold is kept when going from **1** to **2** (Figure S1a,c), it is interesting to note that adjacent chains are oriented with respect to each other in such a way to form an angle of ca. 77° in **1**, but much closer to 90° in **2** (ca. 87°) (Figure S1b,d). Anion– π -type interactions between the perchlorate anions and the bpm aromatic system [$\text{O}_{\text{perchlorate}}\cdots\text{ring}$ centroid distances in the ranges of ca. $3.2(1)$ – $3.4(1)$ Å (**1**) and $3.1(1)$ – $3.5(1)$ Å (**2**)] are also observed in both cases (Figure S2, Supporting Information),

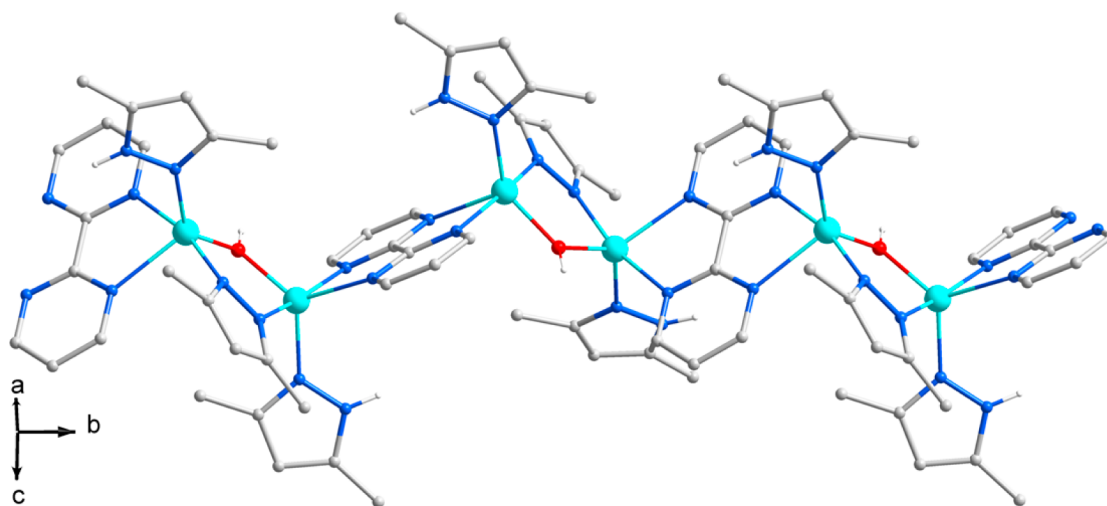


Figure 4. Perspective view of the zigzag cationic $\{[\text{Cu}_2(\mu\text{-OH})(\mu\text{-}3,5\text{-Me}_2\text{pz})(\mu\text{-bpm})(\text{H-}3,5\text{-Me}_2\text{pz})_2]\}^+_n$ chain motif in **3** growing along the crystallographic c axis.

and they are determinant for the generation of the supra-molecular layered network in **2**, but not in **1**.

$\{[\text{Cu}_2(\mu\text{-OH})(\mu\text{-}3,5\text{-Me}_2\text{pz})(\mu\text{-bpm})(\text{H-}3,5\text{-Me}_2\text{pz})_2](\text{ClO}_4)_2\}_n$ (**3**). The crystal structure of **3** is made up by zigzag cationic copper(II) chains of the formula $\{[\text{Cu}_2(\mu\text{-OH})(\mu\text{-}3,5\text{-Me}_2\text{pz})(\mu\text{-bpm})(\text{H-}3,5\text{-Me}_2\text{pz})_2]\}^+_n$, featuring regular alternating bpm and double (3,5-dimethylpyrazolate)(hydroxo) bridges. Monodentate H-3,5-Me₂pz pyrazole groups fill up the coordination sphere at each copper(II) ion, the electroneutrality being achieved by perchlorate counteranions. The two alternating bridging skeletons put adjacent copper(II) ions at intrachain distances of 5.7673(7) Å [across the bis-bidentate bpm] and 3.3220(6) Å [through the (3,5-Me₂pz)(hydroxo) bridge], values that are very close to those found in **1** and **2**. A fragment of the chain in **3** is shown in Figure 4.

The two crystallographically independent copper(II) ions [Cu(1) and Cu(2)] in **3** are both five-coordinate with a CuN₄O chromophore being built by one oxygen atom from the μ -hydroxo bridge and four nitrogen atoms, two from the bis-chelating bpm, one from the bridging 3,5-Me₂pz group, and the remaining one from the neutral monodentate H-3,5-Me₂pz molecule (Figure 5). The values of τ are 0.52 and 0.70 for Cu(1) and Cu(2), respectively, indicating that the geometry around Cu(1) is intermediate between square-pyramidal and trigonal-bipyramidal, whereas that around Cu(2) can be considered in a distorted trigonal-bipyramidal environment. The coexistence in **3** of the H-3,5-Me₂pz molecule and its deprotonated 3,5-Me₂pz form as ligands is most likely due to the enhanced basicity of the 3,5-Me₂pz anion because of the electron-donating character of the methyl substituents (see Discussion above).

The trigonal axis around each copper(II) ion within the $[\text{Cu}^{\text{II}}_2(\mu\text{-OH})(\mu\text{-}3,5\text{-Me}_2\text{pz})]$ fragment of **3** [N(1)–Cu(1)–N(5) and N(4a)–Cu(2)–N(6)] lies in the mean plane of the bridging 3,5-Me₂pz group (Figure 5a), the trigonal mean plane at each copper center forming dihedral angles with the mean plane of the pyrazolate ring of ca. 70° [Cu(1)] and 99° [Cu(2)]. The value of the Cu–N–N–Cu torsion angle (γ) at the pyrazolate bridge is 26.5(3)°, while the Cu–O–Cu interbond angle (α) with the hydroxide supporting bridge is 120.9(1)°. This last value compares well with those found in the related (pyrazolate)(hydroxo)-bridged dinuclear copper(II)

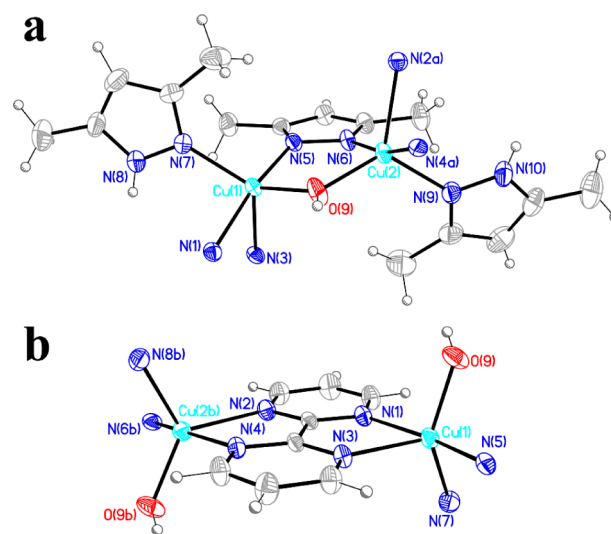


Figure 5. Comparative views of the two alternating bridging moieties in **3**, showing the atom numbering: (a) ($\mu\text{-}3,5\text{-Me}_2\text{pyrazolate})(\mu\text{-hydroxo})$ dicopper(II) and (b) ($\mu\text{-bipyrimidine})$ dicopper(II) units. Thermal ellipsoids are drawn at the 30% probability level. Symmetry operations used to generate equivalent atoms: (a) $-x + 3/2, y + 1/2, z$; (b) $-x + 3/2, y - 1/2, z$.

complexes ($\alpha = 117.5\text{--}123.9^\circ$).^{27q,r,w} These structural features lead to an overall *quasi*-planar conformation of the resulting five-membered metallacyclic core at the ($\mu\text{-pyrazolate})(\mu\text{-hydroxo})$ dicopper(II) unit in **3**, a situation which contrasts with the bent conformation of the six-membered metallacyclic core at the bis($\mu\text{-pyrazolate})(\mu\text{-aqua})$ entity in **1** and **2**. Looking at the ($\mu\text{-bpm})$ dicopper(II) fragment in **3**, the trigonal axes of the copper(II) ions are basically parallel, the trigonal planes of the metal centers forming a dihedral angle of ca. 8.6° (Figure 5b).

The structural differences between **1/2** and **3** are indeed noteworthy. First, there is the aspect of the 1D motif, wavelike (**1/2**) versus zigzag (**3**). Second, in the lack of free water molecules for **3**, the interchain interactions are dominated by N–H⋯O_{perchlorate}⁻ and O–H⋯O_{perchlorate}⁻ type hydrogen bonds involving the terminally bound H-3,5-Me₂pz ligands, the bridging hydroxo group, and the perchlorate counteranions

[N(8)–H(8B)⋯O(5a) = 2.857(5) Å, N(10)–H(10D)⋯O(1b) = 2.850(5) Å, O(9)–H(9)⋯O(4) = 3.240(9) Å, and O(9)–H(9)⋯O(8) = 3.096(8) Å; symmetry code: (a) = $-x + 3/2, y - 1/2, z$; (b) = $-x + 3/2, y + 1/2, z$] (Figure S3, Supporting Information). Weak anion– π -type interactions involving these hydrogen-bonded perchlorate groups and the bpm aromatic system are also observed, as in **1** and **2** [O_{perchlorate}⋯ring centroid distances in the range of ca. 3.2(1)–3.5(1) Å]. However, the copper(II) chains in **3** are well-separated from each other in the plane perpendicular to the propagation direction (Figure S3b), in contrast to what occurs in **1/2** where adjacent chains are connected into intersected supramolecular layers by means of noncovalent interactions in the two perpendicular directions to that of the chain growing.

Magnetic Properties. The magnetic properties of **1–3** in the form of both χ_M and $\chi_M T$ vs T plots [χ_M being the molar magnetic susceptibility per dicopper(II) unit] are shown in Figure 6. At room temperature, the values of $\chi_M T$ are 0.45 (**1** and **2**) and 0.67 cm³ mol⁻¹ K (**3**) (Figure 6b). They are well below that expected for two magnetically isolated copper(II) ions [$\chi_M T = (2N\beta^2 g^2/3k)S_{Cu}(S_{Cu} + 1) = 0.83$ cm³ mol⁻¹ K with $S_{Cu} = 1/2$ and $g = 2.1$]. Upon cooling, the values of $\chi_M T$ decrease continuously from room temperature and those of χ_M

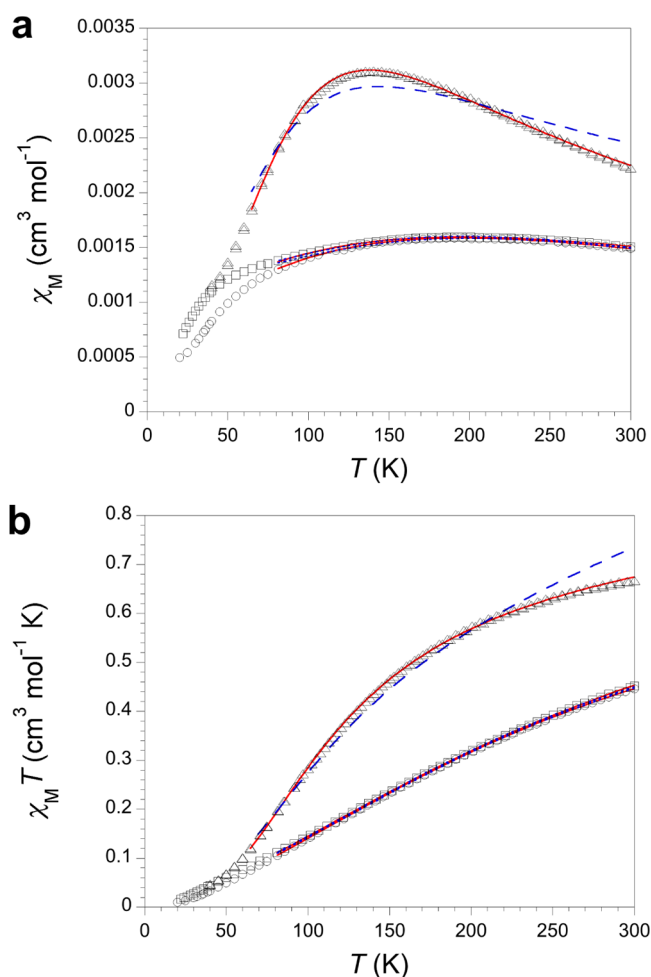


Figure 6. Temperature dependence of χ_M (a) and $\chi_M T$ (b) for **1** (○), **2** (□), and **3** (Δ). The solid red lines are the best-fit curves through the alternating copper(II) chain model, whereas the dotted and dashed blue lines correspond to the uniform copper(II) chain and dinuclear copper(II) models, respectively (see text).

exhibit more or less rounded maxima around 200 K (**1** and **2**) and 140 K (**3**) (Figure 6a). These features are typical of an overall antiferromagnetic behavior.

Having in mind the regular alternating character of the copper(II) chains in **1–3**, their magnetic data were analyzed through the isotropic spin Hamiltonian for an alternating antiferromagnetic copper(II) chain model given by eq 1 (with $\alpha = J'/J$ and $S_i = S_{Cu} = 1/2$)

$$H = -J \sum_{i=1-n/2} (S_{2i} \cdot S_{2i-1} + \alpha S_{2i} \cdot S_{2i+1}) + g\beta H \sum_{i=1-n/2} S_{2i} \quad (1)$$

where J and J' ($J' = \alpha|J|$) are the magnetic coupling constants between the neighboring copper(II) ions within the chain and g is the average Landé factor of the copper(II) ions. The results of the least-squares fit of the magnetic data through the expressions derived by Hatfield for the cases $0 \leq \alpha \leq 0.4$ (**3**) and $0.4 < \alpha \leq 1$ (**1** and **2**) (eqs 2.1–2.7 and 3.1–3.7 respectively, where $x = |J|/2kT$ with $J < 0$ and $J' < 0$)³⁶ are listed in Table 5.

$$\chi_M = (2N\beta^2 g^2/kT)(A + Bx + Cx^2) / (1 + Dx + Ex^2 + Fx^3) \quad (2.1)$$

$$A = 0.25 \quad (2.2)$$

$$B = -0.12587 + 0.22752\alpha \quad (2.3)$$

$$C = 0.019111 - 0.13307\alpha + 0.50967\alpha^2 - 1.3167\alpha^3 + 1.0081\alpha^4 \quad (2.4)$$

$$D = 0.10772 + 1.4192\alpha \quad (2.5)$$

$$E = -0.0028521 - 0.42346\alpha + 2.1953\alpha^2 - 0.82412\alpha^3 \quad (2.6)$$

$$F = 0.37754 - 0.067022\alpha + 6.9805\alpha^2 - 21.678\alpha^3 + 15.838\alpha^4 \quad (2.7)$$

$$\chi_M T = (2N\beta^2 g^2/kT)(A + Bx + Cx^2) / (1 + Dx + Ex^2 + Fx^3) \quad (3.1)$$

$$A = 0.25 \quad (3.2)$$

$$B = -0.13695 + 0.26387\alpha \quad (3.3)$$

$$C = 0.017025 - 0.12668\alpha + 0.49113\alpha^2 - 1.1977\alpha^3 + 0.87257\alpha^4 \quad (3.4)$$

$$D = 0.070509 + 1.3042\alpha \quad (3.5)$$

$$E = -0.0035767 - 0.40837\alpha + 3.4862\alpha^2 - 0.73888\alpha^3 \quad (3.6)$$

$$F = 0.36184 - 0.065528\alpha + 6.65875\alpha^2 - 20.945\alpha^3 + 15.425\alpha^4 \quad (3.7)$$

The theoretical curves for **1–3** (solid lines in Figure 6a,b) closely match the experimental data in the temperature range for which the Hatfield expressions are valid [i.e., for $T \geq |J|/4k \approx 80$ K (**1** and **2**) and 60 K (**3**)].³⁶ In particular, they reproduce perfectly well the rounded maxima of χ_M around 200 K for **1** and **2** (Figure 6a). As a matter of fact, the calculated $-J$ values obtained from the fit of the magnetic susceptibility data of **1**

Table 5. Least-Squares Best-Fit Magnetic Parameters for 1–3

compound	J^a/cm^{-1}	J'^a/cm^{-1}	α^a	g^b	$R^c (\times 10^5)$
1	–217	–211	0.97	2.129	0.3
	(–216)		1	(2.129)	(0.5)
2	–215	–213	0.99	2.126	0.4
	(–214)		1	(2.126)	(0.4)
3	–153	–44	0.30	2.198	0.5
	(–166)		0	(1.794)	(3.1)

^aIntrachain magnetic coupling parameters in the spin Hamiltonian for an alternating copper(II) chain model (eq 1 with $\alpha = J'/J$). The corresponding values for the uniform copper(II) chain and dinuclear copper(II) models (eq 1 with $\alpha = 1$ and 0) are given in parentheses. ^bAverage Landé factor of the Cu^{II} ions. ^cAgreement factor defined as $R = \sum[(\chi_M T)_{\text{exp}} - (\chi_M T)_{\text{calcd}}]^2 / \sum[(\chi_M T)_{\text{exp}}]^2$.

and **2** through the Hatfield expressions agree rather well with those estimated from the temperature of the maxima through the expression $kT_{\text{max}}/|J| = 0.641$ for a uniform copper(II) chain,³⁷ as expected because of the calculated α values close to unity using the alternating copper(II) chain model described above [$\alpha = 0.97$ (**1**) and 0.99 (**2**)]. Indeed, the magnetic properties of **1** and **2** can be also reproduced by considering a uniform copper(II) chain model (eq 1 with $\alpha = 1$) (see Table 5). Therefore, the least-squares fits of the magnetic susceptibility data of **1** and **2** through the appropriate expression developed by Bonner and Fisher (eq 4, where $x = |J|/2kT$ with $J < 0$)³⁷ deviate only slightly from those obtained through the Hatfield expression (dotted lines in Figure 6).

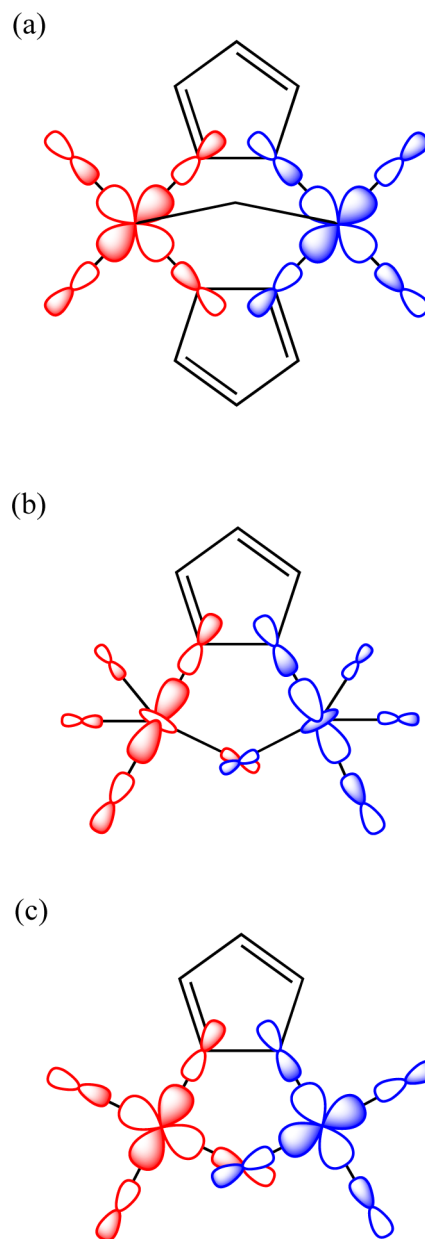
$$\chi_M = (2N\beta^2 g^2/kT)(0.25 + 0.074975x + 0.075235x^2) / (1 + 0.9931x + 0.172135x^2 + 0.757825x^3) \quad (4)$$

On the other hand, attempts to fit the magnetic susceptibility data of **3** through the well-known Bleaney–Bowers expression (eq 5)³⁸ for a dinuclear copper(II) model (eq 1 with $\alpha = 0$) failed (see Table 5) and the best-fit theoretical curve largely deviate from that obtained through the Hatfield expression (dashed line in Figure 6). This is as expected given the calculated α value largely different from zero for **3** using the alternating copper(II) chain model described above ($\alpha = 0.30$).

$$\chi_M = (2N\beta^2 g^2/kT) / [3 + \exp(-J/kT)] \quad (5)$$

Finally, in order to account for the size and nature of the intrachain magnetic couplings in **1–3**, we will focus on the dicopper(II) fragments with the two types of bridges, bpm on one hand and bis(pyrazolate)(aqua) (**1** and **2**) or (pyrazolate)-(hydroxo) (**3**) on the other one.^{26–28} Therefore, the strongest antiferromagnetic couplings in **1** and **2** [$-J = 217$ (**1**) and 215 cm^{-1} (**2**)] are attributed to the bis(μ -pyrazolate)(μ -aqua) pathway present in these two chains, their magnitude being within the range of those previously reported for the related bis(μ -pyrazolate)dicopper(II) complexes with a similar bent conformation ($-J = 143\text{--}330 \text{ cm}^{-1}$), independent on the presence of an additional bridging ligand providing an axial exchange pathway.^{28a,b,1} However, a shift of this range toward stronger antiferromagnetic coupling has been observed for the analogous bis(μ -pyrazolate)dicopper(II) complexes with ancillary chelating arms at the 3- and/or 5-positions of the pyrazolate moiety that possess instead a nearly planar conformation ($-J = 151\text{--}428 \text{ cm}^{-1}$).^{27u,28c–1} This situation can be understood by considering the σ -type equatorial/basal

pathway for the transmission of the electron exchange interaction in **1** and **2**. This pathway involves the pair of $d(x^2-y^2)$ magnetic orbitals that describe the unpaired electrons of the two copper(II) ions that are partially delocalized on the bridging pyrazolate ligands (Scheme 1a). The greater the

Scheme 1. Illustration of the Magnetic Orbitals Centered on Each Metal Ion for Bis(pyrazolate)(aqua)- (a) and (Pyrazolate)(hydroxo)-Bridged (b, c) Dicopper(II) Units of 1–3 with Square-Pyramidal (a, c) and Trigonal-Bipyramidal (b) Metal Environments

deviations from planarity of the bis(μ -pyrazolate)dicopper(II) skeleton are, the smaller the spin delocalization on the bridge, and consequently, the lower the overlap between the magnetic orbitals. As the antiferromagnetic coupling in a dicopper(II) unit is roughly proportional to the square of the integral overlap,^{28l} the deviations from planarity in such a unit would cause a weakening of the antiferromagnetic coupling, as observed.

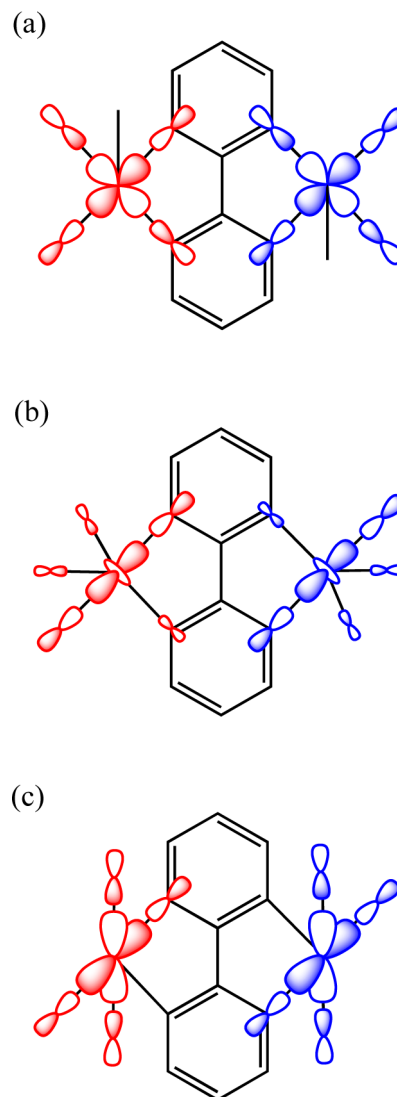
Dealing with the moderate antiferromagnetic coupling across the (μ -pyrazolate)(μ -hydroxo) pathway found for **3** ($-J = 153 \text{ cm}^{-1}$), it is clear that this value is weaker than the strong to very strong antiferromagnetic couplings previously reported for the other dicopper(II) complexes with the same bridging skeleton ($-J = 220\text{--}770 \text{ cm}^{-1}$).^{27q,r,w} This weakening of the antiferromagnetic coupling in **3** can be explained by the different nature of the magnetic orbitals involved in each case. Therefore, the unpaired electron at each copper(II) in **3** is mostly defined by a $d(z^2)$ magnetic orbital that is mainly delocalized on the pyrazolate bridging ligand with only a small spin density on the hydroxo group (Scheme 1b). In the other cases, the magnetic exchange pathway involves the $d(x^2-y^2)$ magnetic orbitals centered on each square-pyramidal Cu^{II} ion and largely delocalized on both the pyrazolate and the hydroxo bridges (Scheme 1c).^{27q,r,w} In this situation, an increase of the overlap between the magnetic orbitals at the supporting hydroxide bridge occurs, and then, the antiferromagnetic coupling is strengthened, as expected for the large values of the Cu–O–Cu angles ($\alpha = 121.2\text{--}123.9^\circ$).^{27q,r,w}

On the other hand, the strong antiferromagnetic coupling through the bis-bidentate bpm in **1** and **2** [$-J' = 211$ (**1**) and 213 cm^{-1} (**2**)] agrees with that previously reported for related symmetric bpm-bridged dicopper(II) complexes ($-J' = 139\text{--}236 \text{ cm}^{-1}$).^{26a-c,e,g-j} Again, the good σ in-plane overlap between the two $d(x^2-y^2)$ magnetic orbitals centered on each Cu^{II} ion and partly delocalized on the bridging skeleton of the symmetric bis-chelating mode of the bpm bridge (Scheme 2a) accounts for this important antiferromagnetic interaction between copper(II) ions separated by more than 5.5 \AA . The much weaker antiferromagnetic coupling through the bpm bridge in **3** ($-J' = 44 \text{ cm}^{-1}$) can be explained in terms of the switching from $d(x^2-y^2)$ magnetic orbitals in **1** and **2** to $d(z^2)$ in **3**.^{26d,f} The magnetic orbitals in **3** are mainly delocalized on the two opposite pyrimidine rings of the bpm bridge with a small, but nonnegligible delocalization, on the other one (Scheme 2b). An overall decrease of the overlap between the magnetic orbitals is predicted, and then, a weaker antiferromagnetic interaction would result, as observed. As a matter of fact, the reduction of the antiferromagnetic coupling is even greater for related asymmetrically bpm-bridged dicopper(II) complexes ($-J = 19 \text{ cm}^{-1}$) possessing a square-pyramidal environment at each metal center and a perpendicular orientation of the basal planes with respect to the mean plane of the bpm bridge (Scheme 2c).^{26d} This is a case of orbital reversal where the spin delocalization of the $d(x^2-y^2)$ magnetic orbitals on each metal ion are exclusively limited to one of the two opposite pyrimidine rings of the bpm bridge. An almost zero overlap between the magnetic orbitals is predicted, and then, a small antiferromagnetic coupling would be involved, as confirmed by the experimental data.

CONCLUSIONS

In this work, we provide a comparative magneto-structural study of three heteroleptic copper(II) compounds, where a series of polymethyl-substituted pyrazoles/pyrazolates and 2,2'-bipyrimidine as well as different exogenous groups act as terminal and/or bridging ligands in a variety of ways, leading thus to different structures and magnetic properties. They include three copper(II) chains with regular alternating bpm and either bis(pyrazolate)(aqua) (**1** and **2**) or (pyrazolate)-(hydroxo) (**3**) bridges. Strong (**1** and **2**) to moderate (**3**) antiferromagnetic couplings are observed within the mono- or

Scheme 2. Illustration of the Magnetic Orbitals Centered on Each Metal Ion for Symmetric (a) and Asymmetric (b, c) bpm-Bridged Dicopper(II) Units of 1–3 with Square-Pyramidal (a, c) and Trigonal-Bipyramidal (b) Metal Environments



bis(pyrazolate)(aqua/hydroxo)dicopper(II) bridging unit, $[\text{Cu}^{\text{II}}_2(\text{Me}_x\text{pz})_n\text{X}]$, with bent or planar conformations, respectively, independent on the nature and number of pyrazolate bridges [$n = 2$ (**1** and **2**) or 1 (**3**) with $x = 0$ (**1**), 1 (**2**), or 2 (**3**)] and exogenous bridging ligands [$\text{X} = \text{H}_2\text{O}$ (**1** and **2**) or OH^- (**3**)]. Otherwise, a strong (**1** and **2**) to weak (**3**) antiferromagnetic coupling occurs between the copper(II) ions across the bis-bidentate bpm with coplanar and parallel arrangements of the magnetic orbitals, respectively. Compounds **1–3** constitute thus three new examples of copper(II) chains with regular alternation of polyatomic bridges with intrachain antiferromagnetic interactions. Further extension of the present work to related oxalate- and polymethyl-substituted pyrazolate-bridged, heteroleptic copper(II) compounds with higher dimensionalities and varying topologies is in progress.

■ ASSOCIATED CONTENT

■ Supporting Information

Selected hydrogen bond distances and angles for **1** and **2** (Tables S1 and S2) and crystal packing views of **1–3** (Figures S1–S3). This material is available free of charge via the Internet at <http://pubs.acs.org>.

■ AUTHOR INFORMATION

Corresponding Authors

*E-mail: isabel.castro@uv.es (I.C.).

*E-mail: nadia.marino@unical.it (N.M.).

Notes

The authors declare no competing financial interest.

■ ACKNOWLEDGMENTS

Financial support by the Spanish Ministerio de Ciencia e Innovación through Project CTQ2010-15364 and Generalitat Valenciana (ISIC/2012/002) is gratefully acknowledged. W.P.B. acknowledges the financial support from the Brazilian agency Coordenação de Aperfeiçoamento de Pessoal de Nível Superior (CAPES) and the Programa Hispano-Brasileño PHB2012-0290. Thanks are also extended to the European Commission, FSE (Fondo Sociale Europeo) and Calabria Region for a fellowship grant to N.M.

■ REFERENCES

- (1) (a) Kahn, O. *Molecular Magnetism*; VCH: Weinheim, Germany, 1993. (b) Launay, J. P.; Verdaguer, M. *Electrons in Molecules: From Basic Principles to Molecular Electronics*; Oxford University Press: Oxford, U.K., 2014.
- (2) (a) Willet, R. D.; Gatteschi, D.; Kahn, O., Eds. *Magneto-Structural Correlations in Exchange-Coupled Systems*; NATO ASI Series 140; Reidel: Dordrecht, 1983. (b) Delhaes, P.; Drillon, M., Eds. *Organic and Inorganic Low-Dimensional Crystalline Materials*; NATO ASI Series 168; Plenum: New York, 1987. (c) Georges, R.; Borrás-Almenar, J. J.; Coronado, E.; Curély, J.; Drillon, M. In *Magnetism: Molecules to Materials*; Miller, J. S., Drillon, M., Eds.; Wiley-VCH: Weinheim, 2001; pp 1–43. (d) Renard, J. P.; Regnault, L.-P.; Verdaguer, M. In *Magnetism: Molecules to Materials*; Miller, J. S., Drillon, M., Eds.; Wiley-VCH: Weinheim, 2001; pp 49–93. (e) Bose, S. *Contemp. Phys.* **2007**, *48*, 13–30.
- (3) (a) Caneschi, A.; Gatteschi, D.; Sessoli, R.; Rey, P. *Acc. Chem. Res.* **1989**, *22*, 392–398. (b) Caneschi, A.; Gatteschi, D.; Rey, P. *Prog. Inorg. Chem.* **1991**, *39*, 331–429. (c) Kahn, O. *Adv. Inorg. Chem.* **1995**, *43*, 179–259. (d) Linert, W.; Verdaguer, M., Eds. *Molecular Magnets. Recent Highlights*; Springer-Verlag: Wien, Austria, 2003.
- (4) (a) Lescouezec, R.; Toma, L. M.; Vaissermann, J.; Verdaguer, M.; Delgado, F. S.; Ruiz-Pérez, C.; Lloret, F.; Julve, M. *Coord. Chem. Rev.* **2005**, *249*, 2691–2729. (b) Bogani, L.; Vindigni, A.; Sessoli, R.; Gatteschi, D. *J. Mater. Chem.* **2008**, *18*, 4750–4758. (c) Miyasaka, H.; Julve, M.; Yamashita, M.; Clérac, R. *Inorg. Chem.* **2009**, *48*, 3420–3437. (d) Coronado, E.; Galán-Mascarós, J. R.; Martí-Gastaldo, C. *CrystEngComm* **2009**, *11*, 2143–2153. (e) Sun, H. L.; Wang, M.; Gao, S. *Coord. Chem. Rev.* **2010**, *254*, 1081–1100. (f) Colombo, V.; Galli, S.; Choi, H. J.; Han, G. D.; Maspero, A.; Palmisano, G.; Masciocchi, N.; Long, J. R. *Chem. Sci.* **2011**, *2*, 1311–1319.
- (5) (a) Renard, J. P.; Verdaguer, M.; Regnault, L. P.; Erkelens, W. A. C.; Rossat-Mignod, J.; Stirling, W. G. *Europhys. Lett.* **1987**, *3*, 945–951. (b) Renard, J. P.; Verdaguer, M.; Regnault, L. P.; Erkelens, W. A. C.; Rossat-Mignod, J.; Ribas, J.; Stirling, W. G.; Vettier, C. *J. Appl. Phys.* **1988**, *63*, 3538–3542.
- (6) (a) Zvyagin, S. A.; Wosnitzer, J.; Kolezhuk, A. K.; Krzystek, J.; Feyerherm, R. *J. Phys.: Conf. Ser.* **2006**, *51*, 39–42. (b) Mourigal, M.; Enderle, M.; Klöpperpieper, A.; Caux, J.-S.; Stunault, A.; Ronnow, H. M. *Nat. Phys.* **2013**, *9*, 435–441.
- (7) (a) Brukner, C.; Vedral, V.; Zeilinger, A. *Phys. Rev. A* **2006**, *73*, 012110. (b) Hao, X.; Zhu, S. *Int. J. Quantum Inf.* **2006**, *04*, 1037–1047.
- (8) Chen, C.-T.; Suslick, K. S. *Coord. Chem. Rev.* **1993**, *128*, 293–322.
- (9) Adhikary, C.; Koner, S. *Coord. Chem. Rev.* **2010**, *254*, 2933–2958.
- (10) (a) De Munno, G.; Julve, M.; Lloret, F.; Faus, J.; Verdaguer, M.; Caneschi, A. *Angew. Chem., Int. Ed. Engl.* **1993**, *32*, 1046–1048. (b) Julve, M.; Verdaguer, M.; De Munno, G.; Real, J. A.; Bruno, G. *Inorg. Chem.* **1993**, *32*, 795–802. (c) De Munno, G.; Bazzicalupi, C.; Faus, J.; Lloret, F.; Julve, M. *J. Chem. Soc., Dalton Trans.* **1994**, 1879–1884. (d) De Munno, G.; Julve, M.; Lloret, F.; Faus, J.; Verdaguer, M.; Caneschi, A. *Inorg. Chem.* **1995**, *34*, 157–165. (e) De Munno, G.; Poerio, T.; Julve, M.; Lloret, F.; Faus, J.; Caneschi, A. *J. Chem. Soc., Dalton Trans.* **1998**, 1679–1685. (f) Marino, N.; Armentano, D.; De Munno, G.; Cano, J.; Lloret, F.; Julve, M. *Inorg. Chem.* **2012**, *51*, 4323–4334.
- (11) (a) Grove, H.; Sletten, J.; Julve, M.; Lloret, F.; Lezama, L. *Inorg. Chim. Acta* **2000**, *310*, 217–226. (b) Grove, H.; Sletten, J.; Julve, M.; Lloret, F.; Cano, J. *J. Chem. Soc., Dalton Trans.* **2001**, 259–265. (c) Yuste, C.; Cañadillas-Delgado, L.; Ruiz-Pérez, C.; Lloret, F.; Julve, M. *Dalton Trans.* **2010**, 167–179.
- (12) Mastropietro, T. F.; Armentano, D.; Grisolia, E.; Zanchini, C.; Lloret, F.; Julve, M.; De Munno, G. *Dalton Trans.* **2008**, 514–520.
- (13) Marinho, M. V.; Marques, L. F.; Diniz, R.; Stumpf, H. O.; Visentin, L. D.; Yoshida, M. I.; Machado, F. C.; Lloret, F.; Julve, M. *Polyhedron* **2012**, *45*, 1–8.
- (14) (a) Hernández-Molina, M.; González-Platas, J.; Ruiz-Pérez, C.; Lloret, F.; Julve, M. *Inorg. Chim. Acta* **1999**, *284*, 258–265. (b) Grove, H.; Sletten, J.; Julve, M.; Lloret, F. *J. Chem. Soc., Dalton Trans.* **2001**, 2487–2493.
- (15) (a) Thompson, L. K.; Tandon, S. S.; Lloret, F.; Cano, J.; Julve, M. *Inorg. Chem.* **1997**, *36*, 3301–3306. (b) De Munno, G.; Lombardi, M. G.; Julve, M.; Lloret, F.; Faus, J. *Inorg. Chim. Acta* **1998**, *282*, 82–89. (c) De Munno, G.; Lombardi, M. G.; Paoli, P.; Lloret, F.; Julve, M. *Inorg. Chim. Acta* **1998**, *282*, 252–256. (d) Carranza, J.; Sletten, J.; Lloret, F.; Julve, M. *J. Mol. Struct.* **2008**, *890*, 31–40. (e) Mastropietro, T. F.; Marino, N.; Armentano, D.; De Munno, G.; Yuste, C.; Lloret, F.; Julve, M. *Cryst. Growth Des.* **2013**, *13*, 270–281.
- (16) (a) De Munno, G.; Bruno, G.; Nicolo, F.; Julve, M.; Real, J. A. *Acta Crystallogr.* **1993**, *C49*, 457–460. (b) Carranza, J.; Sletten, J.; Lloret, F.; Julve, M. *Polyhedron* **2009**, *28*, 2249–2257.
- (17) (a) Vangdal, B.; Carranza, J.; Lloret, F.; Julve, M.; Sletten, J. *J. Chem. Soc., Dalton Trans.* **2002**, 566–574. (b) Carranza, J.; Brennan, C.; Sletten, J.; Lloret, F.; Julve, M. *J. Chem. Soc., Dalton Trans.* **2002**, 3164–3170. (c) Carranza, J.; Sletten, J.; Lloret, F.; Julve, M. *Inorg. Chim. Acta* **2004**, *357*, 3304–3316.
- (18) (a) Yuste, C.; Bentama, A.; Stiriba, S.-E.; Armentano, D.; De Munno, G.; Lloret, F.; Julve, M. *Dalton Trans.* **2007**, 5190–5200. (b) Yuste, C.; Armentano, D.; Marino, N.; Cañadillas-Delgado, L.; Delgado, F. S.; Ruiz-Pérez, C.; Rillema, D. P.; Lloret, F.; Julve, M. *Dalton Trans.* **2008**, 1583–1596. (c) Yuste, C.; Gomes, D. C. D.; Adams, H.; Thomas, J. A.; Lloret, F.; Julve, M. *Polyhedron* **2008**, *27*, 2577–2584.
- (19) Yuste, C.; Bentama, A.; Marino, N.; Armentano, D.; Setifi, F.; Triki, I.; Lloret, F.; Julve, M. *Polyhedron* **2009**, *28*, 1287–1294.
- (20) Sertucha, J.; Luque, A.; Castillo, O.; Román, P.; Lloret, F.; Julve, M. *Inorg. Chem. Commun.* **1999**, *2*, 14–16.
- (21) (a) Castillo, O.; Luque, A.; Julve, M.; Lloret, F.; Román, P. *Inorg. Chim. Acta* **2001**, *315*, 9–17. (b) Castillo, O.; Luque, A.; Román, P.; Lloret, F.; Julve, M. *Inorg. Chem.* **2001**, *40*, 5526–5535. (c) Carranza, J.; Grove, H.; Sletten, J.; Lloret, F.; Julve, M.; Krüfer, P. E.; Eller, C.; Rillema, D. P. *Eur. J. Inorg. Chem.* **2004**, 4836–4848. (d) Vilela, R. S.; Oliveira, T. L.; Martins, F. T.; Ellena, J. A.; Lloret, F.; Julve, M.; Cangussu, D. C. R. *Chim.* **2012**, *15*, 856–865.
- (22) (a) Lloret, F.; Julve, M.; Faus, J.; Journaux, Y.; Philoche-Levisalles, M.; Jeannin, Y. *Inorg. Chem.* **1989**, *28*, 3702–3706. (b) Lloret, F.; Sletten, J.; Ruiz, R.; Julve, M.; Faus, J.; Verdaguer, M. *Inorg. Chem.* **1992**, *31*, 778–784. (c) Lloret, F.; Julve, M.; Faus, J.

- Ruiz, R.; Castro, I.; Mollar, M.; Philoche-Levisalles, M. *Inorg. Chem.* **1992**, *31*, 784–791. (d) Lloret, F.; Julve, M.; Real, J. A.; Faus, J.; Ruiz, R.; Mollar, M.; Castro, I.; Bois, C. *Inorg. Chem.* **1992**, *31*, 2956–2961. (e) Real, J. A.; Ruiz, R.; Faus, J.; Lloret, F.; Julve, M.; Journaux, Y.; Philoche-Levisalles, M.; Bois, C. *J. Chem. Soc., Dalton Trans.* **1994**, 3769–3773. (f) Sanz, J. L.; Cervera, B.; Ruiz, R.; Bois, C.; Faus, J.; Lloret, F.; Julve, M. *J. Chem. Soc., Dalton Trans.* **1996**, 1359–1366. (g) Castro, I.; Calatayud, M. L.; Sletten, J.; Julve, M.; Lloret, F. *C. R. Acad. Sci., Ser. IIC: Chim.* **2001**, *4*, 235–243. (h) Simoes, T. R. G.; Do Pim, W. D.; Silva, I. F.; Oliveira, W. X. C.; Pinheiro, C. B.; Pereira, C. L. M.; Lloret, F.; Julve, M.; Stumpf, H. O. *CrystEngComm* **2013**, *15*, 10165–10170.
- (23) (a) Ruiz-Pérez, C.; Sanchiz, J.; Hernández-Molina, M.; Lloret, F.; Julve, M. *Inorg. Chem.* **2000**, *39*, 1363–1370. (b) Ruiz-Pérez, C.; Hernández-Molina, M.; Lorenzo-Luis, P.; Lloret, F.; Cano, J.; Julve, M. *Inorg. Chem.* **2000**, *39*, 3845–3852. (c) Sanchiz, J.; Rodríguez-Martín, Y.; Ruiz-Pérez, C.; Mederos, A.; Lloret, F.; Julve, M. *New J. Chem.* **2002**, *26*, 1624–1628. (d) Pasán, J.; Sanchiz, J.; Ruiz-Pérez, C.; Lloret, F.; Julve, M. *Eur. J. Inorg. Chem.* **2004**, 4081–4090. (e) Pasán, J.; Sanchiz, J.; Cañadillas-Delgado, L.; Fabelo, O.; Deniz, M.; Lloret, F.; Julve, M.; Ruiz-Pérez, C. *Polyhedron* **2009**, *28*, 1802–1807. (f) Delgado, F. S.; Jimenez, C. A.; Lorenzo-Luis, P.; Pasán, J.; Fabelo, O.; Cañadillas-Delgado, L.; Lloret, F.; Julve, M.; Ruiz-Pérez, C. *Cryst. Growth Des.* **2012**, *12*, 599–614.
- (24) (a) Ehlert, M. K.; Rettig, S. J.; Storr, A.; Thompson, R. C.; Trotter, J. *Can. J. Chem.* **1989**, *67*, 1970–1974. (b) Ehlert, M. K.; Rettig, S. J.; Storr, A.; Thompson, R. C.; Trotter, J. *Can. J. Chem.* **1991**, *69*, 432–439. (c) Ehlert, M. K.; Rettig, S. J.; Storr, A.; Thompson, R. C.; Trotter, J. *Can. J. Chem.* **1992**, *70*, 1121–1128.
- (25) (a) Vecchio-Sadus, A. M. V. *Transition Met. Chem.* **1995**, *20*, 46–55. (b) Sadus, A. M. V. *Transition Met. Chem.* **1995**, *20*, 46–55. (c) Masciocchi, N.; Ardizzoia, G. A.; Brenna, S.; LaMonica, G.; Maspero, A.; Galli, S.; Sironi, A. *Inorg. Chem.* **2002**, *41*, 6080–6089.
- (26) (a) De Munno, G.; Bruno, G. *Acta Crystallogr.* **1984**, *C40*, 2030–2032. (b) Julve, M.; De Munno, G.; Bruno, G.; Verdager, M. *Inorg. Chem.* **1988**, *27*, 3160–3165. (c) Spek, A. L. *Acta Crystallogr.* **1990**, *A46*, c34–c37. (d) De Munno, G.; Julve, M.; Verdager, M.; Bruno, G. *Inorg. Chem.* **1993**, *32*, 2215–2220. (e) Castro, I.; Sletten, J.; Glærum, F.; Lloret, F.; Faus, J.; Julve, M. *J. Chem. Soc., Dalton Trans.* **1994**, 2777–2782. (f) De Munno, G.; Julve, M.; Lloret, F.; Cano, J.; Caneschi, A. *Inorg. Chem.* **1995**, *34*, 2048–2053. (g) Castro, I.; Sletten, J.; Glærum, F.; Cano, J.; Lloret, F.; Faus, J.; Julve, M. *J. Chem. Soc., Dalton Trans.* **1995**, 3207–3213. (h) Kawata, S.; Kumagai, H.; Kitagawa, S.; Honda, K.; Enomoto, M.; Katada, M. *Mol. Cryst. Liq. Cryst. Sci. Technol., Sect. A* **1996**, *286*, 51–58. (i) Rodríguez-Martín, Y.; Sanchiz, J.; Ruiz-Pérez, C.; Lloret, F.; Julve, M. *Inorg. Chim. Acta* **2001**, *326*, 20–26. (j) Thetiot, F.; Triki, S.; Pala, J. S.; Galán-Mascarós, J. R.; Martínez-Agudo, J. M.; Dunbar, K. R. *Eur. J. Inorg. Chem.* **2004**, 3783–3791.
- (27) (a) Mazurek, W.; Kennedy, B. J.; Murray, K. S.; O'Connor, M. J.; Rodgers, J. R.; Snow, M. R.; Wedd, A. G.; Zwack, P. R. *Inorg. Chem.* **1985**, *24*, 3258–3264. (b) Nishida, Y.; Kida, S. *Inorg. Chem.* **1988**, *27*, 447–452. (c) Doman, T. N.; Williams, D. E.; Banks, J. F.; Buchanan, R. M.; Chang, H. R.; Webb, R. J.; Hendrickson, D. N. *Inorg. Chem.* **1990**, *29*, 1058–1062. (d) Baggio, R.; González, O.; Garland, M. T.; Manzur, J.; Acuna, V.; Atria, A. M.; Spodine, E.; Pena, O. *J. Crystallogr. Spectrosc. Res.* **1993**, *23*, 749–753. (e) Nonoyama, K.; Mori, W.; Nakajima, K.; Nonoyama, M. *Polyhedron* **1997**, *16*, 3815–3826. (f) Kruger, P. E.; Launay, F.; McKee, V. *Chem. Commun.* **1999**, 639–640. (g) Spodine, E.; Atria, A. M.; Valenzuela, J.; Jalocho, J.; Manzur, J.; García, A. M.; Garland, M. T.; Peña, O.; Saillard, J. Y. *J. Chem. Soc., Dalton Trans.* **1999**, 3029–3034. (h) Chou, J.-L.; Horng, D.-N.; Chyn, J.-P.; Lee, K. M.; Urbach, F. L.; Lee, G.-H.; Tsai, H.-L. *Inorg. Chem. Commun.* **1999**, *2*, 392–395. (i) Chou, J.-L.; Chyn, J.-P.; Urbach, F. L.; Gervasio, D. F. *Polyhedron* **2000**, *19*, 2215–2223. (j) Iskander, M. F.; Khalil, T. E.; Haase, W.; Werner, R.; Svoboda, I.; Fuess, H. *Polyhedron* **2001**, *20*, 2787–2798. (k) Kara, H.; Elerman, Y.; Prout, K. Z. *Naturforsch., B: J. Chem. Sci.* **2000**, *55*, 796–802. (l) Kara, H.; Elerman, Y.; Prout, K. Z. *Naturforsch., B: J. Chem. Sci.* **2001**, *56*, 719–727. (m) Elerman, Y.; Elmali, A. Z. *Naturforsch., B: J. Chem. Sci.* **2001**, *56*, 970–974. (n) Elerman, Y.; Kara, H.; Elmali, A. Z. *Naturforsch., B: J. Chem. Sci.* **2001**, *56*, 1129–1137. (o) Courtney, S. C.; Murray, K. S.; Tiekink, E. R. T. Z. *Kristallogr. - New Cryst. Struct.* **2002**, *217*, 217–218. (p) Elerman, Y.; Kara, H.; Elmali, A. Z. *Naturforsch., A: Phys. Sci.* **2003**, *58*, 363–372. (q) Escrivá, E.; García-Lozano, J.; Martínez-Lillo, J.; Nuñez, H.; Server-Carrió, J.; Soto, L.; Carrasco, R.; Cano, J. *Inorg. Chem.* **2003**, *42*, 8328–8336. (r) Zareba, M.; Drabent, K.; Ciunik, Z.; Wolowiec, S. *Inorg. Chem. Commun.* **2004**, *7*, 82–85. (s) Huang, S.-F.; Chou, Y.-C.; Misra, P.; Lee, C.-J.; Mohanta, S.; Wei, H.-H. *Inorg. Chim. Acta* **2004**, *357*, 1627–1631. (t) Mezei, G.; Raptis, R. G. *Inorg. Chim. Acta* **2004**, *357*, 3279–3288. (u) De Geest, D. J.; Noble, A.; Moubaraki, B.; Murray, K. S.; Larsen, D. S.; Brooker, S. *Dalton Trans.* **2007**, 467–475. (v) Roy, P.; Dhara, K.; Manassero, M.; Banerjee, P. *Eur. J. Inorg. Chem.* **2008**, 4404–4412. (w) Singh, A. K.; Van der Vlugt, J. I.; Demeshko, S.; Dechert, S.; Meyer, F. *Eur. J. Inorg. Chem.* **2009**, 3431–3439. (x) Popov, L. D.; Levchenkov, S. I.; Scherbakov, I. N.; Lukov, V. V.; Suponitsky, K. Y.; Kogan, V. A. *Inorg. Chem. Commun.* **2012**, *17*, 1–4. (y) Wei, W.; Xu, Y. *Acta Crystallogr.* **2012**, *E68*, m557–m557.
- (28) (a) Ajò, D.; Bencini, A.; Mani, F. *Inorg. Chem.* **1988**, *27*, 2437–2444. (b) Drew, M. G. B.; Yates, P. C.; Esho, F. S.; Trocha-Grimshaw, J.; Lavery, A.; McKillop, K. P.; Nelson, S. M.; Nelson, J. *J. Chem. Soc., Dalton Trans.* **1988**, 2995–3003. (c) Kamiyuki, T.; Okawa, H.; Matsumoto, N.; Kida, S. *J. Chem. Soc., Dalton Trans.* **1990**, 195–198. (d) Kamiyuki, T.; Okawa, H.; Inoue, H.; Matsumoto, N.; Koda, M.; Kida, S. *J. Coord. Chem.* **1991**, *23*, 201–211. (e) Bayon, J. C.; Esteban, P.; Net, G.; Rasmussen, P. G.; Baker, K. N.; Hahn, C. W.; Gumz, M. M. *Inorg. Chem.* **1991**, *30*, 2572–2574. (f) Pons, J.; López, X.; Casabó, J.; Teixidor, F.; Caubet, A.; Rius, J.; Miravittles, C. *Inorg. Chim. Acta* **1992**, *195*, 61–66. (g) Ehlert, M. K.; Rettig, S. J.; Storr, A.; Thompson, R. C.; Trotter, J. *Can. J. Chem.* **1992**, *70*, 2161–2173. (h) Mernari, B.; Abraham, F.; Lagrenee, M.; Drillon, M.; Legoll, P. *J. Chem. Soc., Dalton Trans.* **1993**, 1707–1711. (i) Degang, F.; Guoxiong, W.; Zongyan, Z.; Xiangge, Z. *Transition Met. Chem.* **1994**, *19*, 592–594. (j) Hanot, V. P.; Robert, T. D.; Kolnaar, J.; Haasnoot, J. G.; Reedijk, J.; Kooijman, H.; Spek, A. L. *J. Chem. Soc., Dalton Trans.* **1996**, 4275–4281. (k) Fleming, J. S.; Psilakis, E.; Jeffery, J. C.; Mann, K. L. V.; McCleverty, J. A.; Ward, M. D. *Polyhedron* **1998**, *17*, 1705–1714. (l) Matsushima, H.; Hamada, H.; Watanabe, K.; Koikawa, M.; Tokii, T. *J. Chem. Soc., Dalton Trans.* **1999**, 971–977. (m) Lamarque, L.; Navarro, P.; Miranda, C.; Aran, V. J.; Ochoa, C.; Escarti, F.; García-España, E.; Latorre, J.; Luis, S. V.; Miravet, J. F. *J. Am. Chem. Soc.* **2001**, *123*, 10560–10570. (n) King, P.; Clerac, R.; Anson, C. E.; Powell, A. K. *Dalton Trans.* **2004**, 852–861. (o) Liu, X.; McAllister, J. A.; De Miranda, M. P.; McInnes, E. J. L.; Kilner, C. A.; Halcrow, M. A. *Chem.—Eur. J.* **2004**, *10*, 1827–1837. (p) Teichgraber, J.; Leibeling, G.; Dechert, S.; Meyer, F. *Z. Anorg. Allg. Chem.* **2005**, *631*, 2613–2618. (q) Denisova, T. O.; Amelchenkova, E. V.; Pruss, I. V.; Dobrokhotova, Z. V.; Fiakovskii, O. P.; Nifedov, S. E. *Russ. J. Inorg. Chem.* **2006**, *51*, 1020–1064. (r) Xing, Y. F.; Zhang, X. J.; Sun, Z.; Han, J.; Zhang, Y. H.; Zhang, B. L.; Ge, M. Y.; Niu, S. Y. *Spectrochim. Acta, Part A* **2007**, *68*, 1256–1262. (s) Mokuolu, Q. F.; Foguet-Albiol, D.; Jones, L. F.; Wolowska, J.; Kowalczyk, R. M.; Kilner, C. A.; Christou, G.; McGowan, P. C.; Halcrow, M. A. *Dalton Trans.* **2007**, 1392–1399. (t) Mishra, V.; Lloret, F.; Mukherjee, R. *Eur. J. Inorg. Chem.* **2007**, 2161–2170. (u) Di Nicola, C.; Marchetti, F.; Monari, M.; Pandolfo, L.; Pettinari, C. *Inorg. Chem. Commun.* **2008**, *11*, 665–668. (v) Zhang, S.-Y.; Li, Y.; Li, W. *Inorg. Chim. Acta* **2009**, *362*, 2247–2252. (w) Mishima, A.; Fuyuhiko, A.; Kumagai, H.; Kawata, S. *Acta Crystallogr.* **2011**, *E67*, m1523–m1524.
- (29) (a) Castro, I.; Faus, J.; Julve, M.; Lloret, F.; Verdager, M.; Kahn, O.; Jeannin, S.; Jeannin, Y.; Vaisserman, J. *J. Chem. Soc., Dalton Trans.* **1990**, 2207–2212. (b) Angaroni, M. A.; Atdizzoia, G. A.; Beringhelli, T.; La Monica, G.; Gatteschi, D.; Masciocchi, N.; Moret, M. *J. Chem. Soc., Dalton Trans.* **1990**, 3305–3309. (c) Ardizzoia, G. A.; Angaroni, M. A.; La Monica, G.; Cariati, F.; Cenini, S.; Moret, M.; Masciocchi, N. *Inorg. Chem.* **1991**, *30*, 4349–4353.
- (30) SAINT, Version 6.45; Bruker Analytical X-ray Systems Inc: Madison, WI, 2003.

- (31) SADABS, Version 2.03; Bruker AXS Inc.: Madison, WI, 2000.
- (32) Sheldrick, G. M. *Acta Crystallogr.* **2008**, *A64*, 112–122.
- (33) (a) Müller, P. *Cryst. Rev.* **2009**, *15*, 57–83. (b) Müller, P.; Herbst-Irmer, R.; Spek, A. L.; Schneider, T. R.; Sawaya, M. R. *Crystal Structure Refinement: A Crystallographer's Guide to SHELXL*; Müller, P., Ed.; IUCr Texts on Crystallography; Oxford University Press: Oxford, U.K., 2006.
- (34) *DIAMOND 3.1b*; Crystal Impact GbR and Brandenburg & H. Putz GBR: Bonn, Germany, 2006.
- (35) Addison, A. W.; Nageswara, T.; Reedijk, J.; van Rijn, J.; Verschoor, G. C. *J. Chem. Soc., Dalton Trans.* **1984**, 1349–1356.
- (36) Hall, J. W.; Marsh, W. E.; Weller, R. R.; Hatfield, W. E. *Inorg. Chem.* **1981**, *20*, 1033–1037.
- (37) Bonner, J. C.; Fisher, M. E. *Phys. Rev.* **1964**, *135*, A640–658.
- (38) Bleaney, B.; Bowers, K. D. *Proc. R. Soc. London, Ser. A* **1952**, *214*, 451–465.